

Disentangling the rhythms of human activity in the built environment for airborne transmission risk: an analysis of large-scale mobility data

Zachary Susswein¹, Eva C. Rest¹, and Shweta Bansal^{1,*}

¹Department of Biology, Georgetown University, Washington, DC, USA

*Corresponding Author: shweta.bansal@georgetown.edu

December 2022

Abstract

Background Since the outset of the COVID-19 pandemic, substantial public attention has focused on the role of seasonality in impacting transmission. Misconceptions have relied on seasonal mediation of respiratory diseases driven solely by environmental variables. However, seasonality is expected to be driven by host social behavior, particularly in highly susceptible populations. A key gap in understanding the role of social behavior in respiratory disease seasonality is our incomplete understanding of the seasonality of indoor human activity.

Methods We leverage a novel data stream on human mobility to characterize activity in indoor versus outdoor environments in the United States. We use an observational mobile app-based location dataset encompassing over 5 million locations nationally. We classify locations as primarily indoor (e.g. stores, offices) or outdoor (e.g. playgrounds, farmers markets), disentangling location-specific visits into indoor and outdoor, to arrive at a fine-scale measure of indoor to outdoor human activity across time and space.

Results We find the proportion of indoor to outdoor activity during a baseline year is seasonal, peaking in winter months. The measure displays a latitudinal gradient with stronger seasonality at northern latitudes and an additional summer peak in southern latitudes. We statistically fit this baseline indoor-outdoor activity measure to inform the incorporation of this complex empirical pattern into infectious disease dynamic models. However, we find that the disruption of the COVID-19 pandemic caused these patterns to shift significantly from baseline, and the empirical patterns are necessary to predict spatiotemporal heterogeneity in disease dynamics.

Conclusions Our work empirically characterizes, for the first time, the seasonality of human social behavior at a large scale with high spatiotemporal resolution, and provides a parsimonious parameterization of seasonal behavior that can be included in infectious disease dynamics models. We provide critical evidence and methods necessary to inform the public health of seasonal and pandemic respiratory pathogens and improve our understanding of the relationship between the physical environment and infection risk in the context of global change.

Funding Research reported in this publication was supported by the National Institute of General Medical Sciences of the National Institutes of Health under award number R01GM123007.

1 Introduction

The seasonality of infectious diseases is a widespread and familiar phenomenon. Although a number of potential mechanisms driving seasonality in directly transmitted infectious diseases have been proposed, the causal process behind seasonality is still largely an open question [1, 2, 3]. In the case of the influenza virus, seasonal changes in humidity have been identified as a potential mechanism, with drier winter months enhancing transmission [4, 5, 6]; similar patterns have been observed for respiratory syncytial virus and hand

41 foot and mouth disease [7, 8]. However, humidity is but one of many mechanisms contributing to seasonality
42 in infectious disease transmission. Seasonal changes in temperature, human mixing patterns, and the immune
43 landscape, among other factors, are thought to contribute to transmission dynamics [9, 10, 11, 12, 2]. The
44 relative importance of these disparate mechanisms varies across directly-transmitted pathogens and is still
45 largely unexplained [1, 3]. The influence of seasonal host behavior on respiratory disease seasonality remains
46 particularly understudied [13, 11] except for a few notable examples [14, 15, 16].

47 For respiratory pathogens spread via the aerosol transmission route, in particular, seasonality may be medi-
48 ated by multiple behaviorally-driven mechanisms. Aerosol transmission, a significant mode of transmission
49 for a number of respiratory pathogens including tuberculosis, measles, and influenza [17], has become increas-
50 ingly acknowledged during the COVID-19 pandemic [18, 19, 20, 21, 22]. The role of aerosols in respiratory
51 disease transmission allows for transmission outside of the traditional 6 ft. radius and 5-minute duration for
52 the droplet mode and implicates human mixing in indoor locations with poor ventilation as being a high
53 risk for transmission, regardless of the intensity of the social contact. While more is known about the spa-
54 tiotemporal variation in environmental factors such as temperature and humidity in the indoor environment
55 (e.g. [23]) and about the impact these factors have on airborne pathogen transmission (e.g. [24, 25]), limited
56 information is available on rates of human indoor activity and how this varies geographically and seasonally.
57 In the US, most studies quantifying indoor and outdoor time are conducted in the context of air pollutants,
58 suffer from small study sizes, lack spatiotemporal resolution, and are outdated. The most cited estimates
59 originate from the 1980s-90s and estimate that Americans spend upwards of 90% of their time indoors [26];
60 and more recent data agree with these estimates [27, 28]. While it is well understood that seasonal differ-
61 ences and latitude likely affect time spent indoors, little is known of the spatiotemporal variation in indoor
62 activity beyond this one monolithic estimate, vastly limiting our ability to comprehensively characterize the
63 seasonality of airborne disease exposure risk.

64 Because our understanding of the drivers of seasonality for respiratory diseases has been limited, the model-
65 ing of seasonally-varying infectious disease dynamics has been traditionally done using environmental data-
66 driven or phenomenological approaches. Environmental data-driven approaches incorporate seasonality into
67 epidemiological models through environmental correlates of seasonality, such as solar exposure or outdoor
68 temperature [12, 7, 29]. This approach to seasonal dynamics controls for inter-seasonal variation in trans-
69 mission dynamics and measures the strength of correlations between proposed metrics and seasonal variation
70 in force of infection – although the observed relationship is rarely causally relevant for respiratory disease
71 transmission. In contrast, phenomenological models such as seasonal forcing approaches modulate trans-
72 missibility over time without specifying a particular mechanism for this modulation [30, 2]. By applying
73 well-understood functions (such as sine functions), seasonal forcing allows for flexible specification and quan-
74 tification of dynamics, such as periodicity or oscillation damping, and indirectly captures seasonal variation
75 in non-environmental factors such as school mixing. A significant remaining gap in seasonal infectious disease
76 modeling is thus the ability to empirically incorporate spatiotemporal variation in behavioral mechanisms
77 driving seasonality of disease exposure and transmission.

78 Thus, despite the role of the indoor built environment in exposure to the airborne transmission route,
79 seasonal variation in indoor human mixing has not yet been systemically characterized nor integrated into
80 mathematical models of seasonal respiratory pathogens. To address this gap, we construct a novel metric
81 quantifying the relative propensity for human mixing to be indoors at a fine spatiotemporal scale across
82 the United States. We derive this metric using anonymized mobile GPS panel data of visits of over 45
83 million mobile devices to approximately 5 million public locations across the United States. We find a
84 systematic latitudinal gradient, with indoor activity patterns in the northern and southern United States
85 following distinct temporal trends at baseline. However, we find that the COVID-19 pandemic disrupted this
86 structure. Lastly, we fit simple parametric models to incorporate these seasonal activity dynamics into models
87 of infectious disease transmission when indoor activity is expected to be at baseline. Our work provides the
88 evidence and methods necessary to inform the epidemiology of seasonal and pandemic respiratory pathogens
89 and improve our understanding of the relationship between the physical environment and infection risk in
90 light of global change.

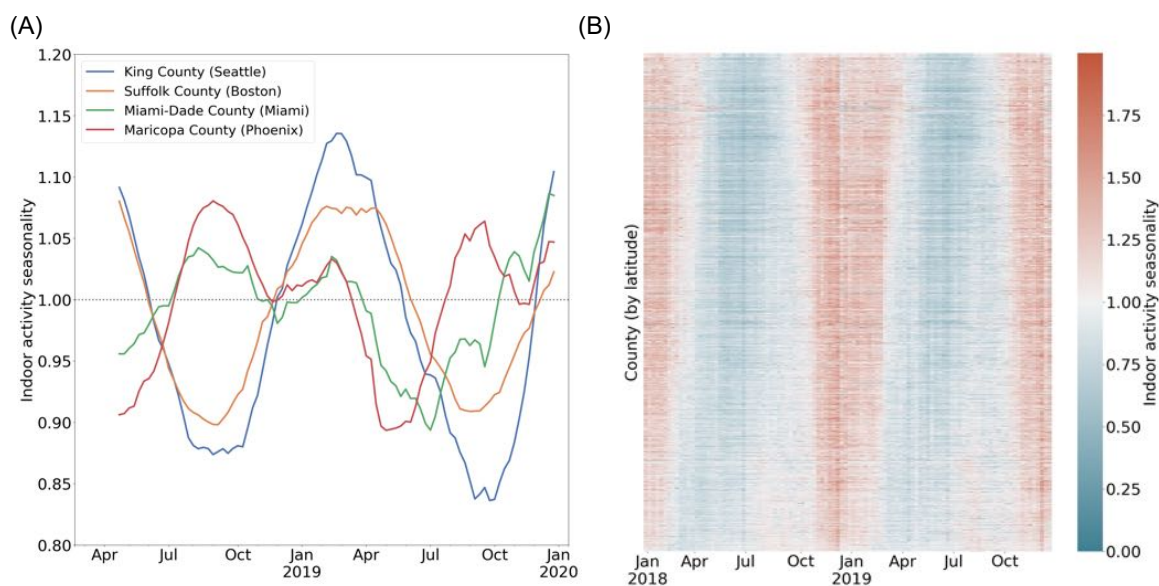


Figure 1: (A) Case studies to highlight varying trends in indoor activity seasonality during 2018 and 2019: King County and Suffolk County (in the northern US) have high indoor activity in the winter months and a trough in indoor activity in the summer months. Miami-Dade and Maricopa County (in the southern US) see moderate indoor activity in the winter and may have an additional peak in indoor activity during the summer. We apply a rolling window mean for visualization purposes. (B) A heatmap of the indoor activity seasonality metric for all US counties by week for 2018 and 2019. Counties are ordered by latitude. We see significant spatiotemporal heterogeneity with distinct trends in the summer versus winter seasons.

91 Methods

92 Data Source

93 We use the SafeGraph Weekly Patterns data, which provides foot traffic at public locations (“points of
94 interest”, referred to as POIs from here on) across the US based on the usage of mobile apps with GPS
95 [31]. The data are from 2018 to 2020, and 4.6 million POIs are sampled in all years of our study. The data
96 is anonymized by applying noise, omitting data associated with a single mobile device, and is provided at
97 the weekly temporal scale. Data are sampled from over 45 million smartphone devices (of approximately
98 275-290 million smartphone devices in the US during 2018-2021 [32]), and does not include devices that are
99 out of service, powered off, or ones that opt out of location services on their devices.

100 This is secondary data analysis, so no informed consent or consent to publish was necessary. Ethical review
101 for this study (STUDY00003041) was sought from the Institutional Review Board at Georgetown University
102 and was approved on October 14, 2020.

103 Defining indoor activity seasonality

104 Safegraph Points of Interest (POIs) are locations where consumers can spend money and/or time and include
105 schools, hospitals, parks, grocery stores, and restaurants, etc, but do not include home locations. (In Figure
106 1—figure supplement 1, we show that time at home does not display significant seasonal variation). Each POI
107 is assigned a six-digit North American Industry Classification System (NAICS) code in the SafeGraph Core
108 Places dataset to classify each location into a business category. We classify each 6-digit NAICS codes (363
109 unique codes in total) as primarily *indoor* (e.g. schools, hospitals, grocery stores), primarily *outdoor* (e.g.
110 parks, cemeteries, zoos). We classify some locations as *unclear* if the location is a potentially mixed indoor
111 and outdoor setting (e.g. gas stations with convenience stores, automobile dealerships). Approximately 90%
112 of POIs were classified as indoors, 6.5% were classified as outdoors, and 3.5% were classified as unclear.
113 In Figure 1—figure supplement 2, we illustrate the robustness of our metric to the classification of unclear
114 locations.

115 We define $\tilde{\sigma}_{it}$, equation (1), as the propensity for visits to be to indoor locations relative to outdoor locations.
116 We aggregated raw visit counts, defined when a device is present at a non-home POI for longer than one
117 minute, to all indoor POIs and all outdoor POIs in a given week (t) at the U.S. county level (i). Visit counts
118 are normalized by the maximum visit counts for indoor or outdoor locations in each county during the year
119 2019. (In Figure 1—figure supplement 3, we show that the max visit count is comparable in 2018 and 2019).

$$\tilde{\sigma}_{it} = \frac{N_{it}^{indoor} / \max_t \{N_{it}^{indoor}\}}{N_{it}^{outdoor} / \max_t \{N_{it}^{outdoor}\}} \quad (1)$$

120 This metric is then mean-centered to arrive at a relative measure of indoor activity seasonality, σ_{it} , which is
121 comparable across all counties:

$$\sigma_{it} = \frac{\tilde{\sigma}_{it}}{\mu_{\tilde{\sigma}}} \quad (2)$$

122 We note that $\mu_{\tilde{\sigma}}$ is not spatially structured (see Figure 2—figure supplement 1).

123 As a data cleaning step, we use spatial imputation for any county-weeks where sample sizes are small. For
124 location-weeks in which the total visit count is less than 100, we impute the indoor activity seasonality using
125 an average of σ in the neighboring locations (where neighbors are defined based on shared county borders).
126 This affects 0.6% of all county-weeks and a total of 79 (out of 3143) counties.

127 Time series clustering analysis

128 To characterize groups of US counties with similar indoor activity dynamics, we use a complex networks-
129 based time series clustering approach. We first calculate the pairwise similarity between z-normalized indoor
130 activity time series for each pair of counties, i and j using the Pearson correlation coefficient (ρ_{ij}). For pairs

131 of locations where ρ_{ij} is in the top 10% of all correlations, we represent the pairwise time series similarities
132 as a weighted network where nodes are US counties and edges represent strong time series similarity. (In
133 Figure 1—figure supplement 4, we show the robustness of our clustering results to this choice of correlation
134 threshold.)

135 We then cluster the time series similarity network using community structure detection. This method
136 effectively clusters nodes (counties) into groups of nodes that are more connected within than between. The
137 resulting clustering thus represents a regionalization of the U.S. in which regions consist of counties that have
138 more similar indoor activity dynamics to each other than to other regions. One benefit of the network-based
139 community detection approach over other clustering methods is that community detection does not require
140 user specification of the number of clusters (regions, in this case); instead the number of clusters emerge
141 organically from the data connectivity [33]. For community detection, we use the Louvain method [34], a
142 multiscale method in which modularity is first optimized using a greedy local algorithm, on the similarity
143 network with edge weights (i.e. time series correlations) using a `igraph` implementation in *Python* [35].

144 We performed a robustness assessment of the community structure using a set of 25 “bootstrap networks”, B_i .
145 For each bootstrap network, the edge weight (i.e. the time series correlation) for each edge of the network was
146 perturbed by $\epsilon N(0, 0.05)$. The community structure algorithm was performed on each bootstrap network. A
147 consensus value was then calculated as the sum of the normalized mutual information between the community
148 structure partition of bootstrap network B_i and all other bootstrap networks. The partition with the largest
149 consensus value was defined as the robust community structure partition.

150 Given some known limitations to the time series correlation network-based approach to clustering [36], we
151 validated our network-based clustering results with another common clustering method. In particular, we
152 used hierarchical clustering with Ward linkage and Euclidean distance on z-normalized indoor activity time
153 series, implemented using `scipy` in *Python*. (We note that Euclidean distance is equivalent to Pearson’s
154 correlation on normalized time series [37]). The results of this comparison are summarized in Figure 1—
155 figure supplement 5.

156 Disruptions to indoor activity due to pandemic response

157 We investigate the COVID-19 pandemic’s impact on indoor activity seasonality by comparing pre-pandemic
158 mobility patterns in 2018 and 2019 with mobility patterns during the COVID-19 pandemic in 2020. We
159 compared the proportion of indoor visits at the county level, σ_{it} , across 2018, 2019, and 2020 to examine
160 changes in indoor activity seasonality during the COVID-19 pandemic. We also examined total activity,
161 aggregating visits to all indoor, outdoor, and unclear POIs by week and mean-centering them for each US
162 county during the COVID-19 pandemic in 2020.

163 Incorporating indoor activity into infectious disease models

164 We seek to illustrate the impact of incorporating seasonality into an infectious disease model using a phe-
165 nomenological model versus empirical data. To achieve this, we parameterize a simple compartmental disease
166 model with a seasonality term, using either our empirically-derived indoor activity seasonality metric or an
167 analytical phenomenological model of seasonality fit to this metric.

168 Phenomenological model of seasonality

169 We first fit our empirically-derived indoor activity seasonality metric using a time-varying non-linear model.
170 We specify the time-varying effect as a sinusoidal function as is commonly done to incorporate seasonality
171 into infectious disease models phenomenologically. The indoor activity seasonality, σ_{it} for cluster i at week
172 t is specified as: $\sigma_{it} = 1 + \alpha_i \sin(\omega_i t + \phi_i)$, where α_i is the sine wave amplitude, ω_i is the frequency and ϕ_i is
173 the phase. We fit a model for locations in the northern cluster separately from those in the southern cluster,
174 as identified above. We fit the parameters for this model using the `nlme`, a standard package in *R* for fitting
175 Gaussian nonlinear models.

176 **Disease model**

We model infectious disease dynamics through a simple SIR model of disease spread:

$$\begin{aligned}\frac{dS}{dt} &= -\beta_0\beta(t)SI \\ \frac{dI}{dt} &= \beta_0\beta(t)SI - \gamma I \\ \frac{dR}{dt} &= \gamma I\end{aligned}$$

177 We incorporate alternative seasonality terms to consider the impact of heterogeneity in indoor seasonality
178 on disease dynamics. For the northern and southern cluster separately, we define modeled seasonality as
179 $\beta(t) = 1 + \alpha \sin(\omega t + \phi)$, with the fitted parameters for each cluster (Figure 4—figure supplement 1 and Figure
180 4—figure supplement 2). We also consider two exemplar locations for empirical estimates of seasonality,
181 where $\beta(t) = \sigma_t$ after rolling window smoothing: Cook County for an example county from the northern
182 cluster, and Maricopa County for an example location from the southern cluster. We also compare against
183 a null expectation where $\beta(t) = 1$. (All seasonality functions are illustrated in Figure 4—figure supplement
184 3). We assume that $\beta_0 = 0.0025$ and $\gamma = 2$ (on a weekly time scale).

185 Results

186 Based on anonymized location data from mobile devices, we construct a novel metric that measures the
187 relative propensity for human activity to be indoors at a fine geographic (US county) and temporal (weekly)
188 scale. Activity is measured as number of visits to unique physical, public (non-residential) locations across
189 the United States. Locations are classified as indoors if they are enclosed environments (i.e. buildings and
190 transportation services). We characterize the systematic spatiotemporal structure in this metric of indoor
191 activity seasonality with a time series clustering analysis. We also characterize the shift that occurred in
192 the baseline patterns of indoor activity seasonality during the COVID-19 pandemic. We note that this
193 seasonal variation in the propensity of human activity to be indoors differs from the variation in overall rates
194 of contact or mobility, which does not appear to be highly seasonal (Figure 1—figure supplement 1, 38).
195 Lastly, we fit non-linear models to the indoor activity metric at baseline, comparing the ability of a simple
196 model to capture seasonal variation in transmission risk.

197 Quantifying empirical dynamics in indoor activity

198 The indoor activity seasonality metric, σ , captures the relative frequency of visits to indoor versus outdoor
199 locations within an area. The components of σ capture the degree to which indoor and outdoor locations
200 are occupied; when $\sigma = 1$, a given county is at its county-specific average propensity (over time) for indoor
201 activity relative to outdoor. When $\sigma < 1$, activity within the county is more frequently outdoor and less
202 frequently indoor than average, while $\sigma > 1$ indicates that activity is more frequently indoor and less
203 frequently outdoor than average. Thus, a σ of 1.2 indicates that the county’s activity is 20% more indoor
204 than average and a σ of 0.80 indicates that the county’s activity is 20% less indoor than average (additional
205 details in methods).

206 Through this metric, we measure the relative propensity for human activity to be indoors for every community
207 (i.e. US county) across time (at a weekly timescale), finding significant heterogeneity between counties
208 (Figure 1A). The representative examples of Cook County, Illinois (home of the city of Chicago in the
209 midwestern US) and Maricopa County, Arizona (home of the city of Phoenix in the southwestern US)
210 highlight systematic spatial and temporal heterogeneity in indoor activity dynamics. In Cook County,
211 indoor activity varies over time, at its peak in the winter, with the relative odds of an indoor visit well
212 above average. During the summer, σ in Cook County reaches its trough, with activity systematically more
213 outdoors on average. On the other hand, the variation of σ across time in Maricopa County is characterized
214 by a smaller winter peak in indoor activity, and an additional peak in the summer (i.e. July and August); this
215 peak occurs concurrently with the trough in Cook County. Unlike in Cook County, σ in Maricopa County is
216 lowest in the spring and fall. These representative counties illustrate the systematic within-county variation
217 in indoor activity over time, as well as the between-county variation in temporal trends as represented in
218 Figure 1B for all US communities.

219 To identify systematic geographic structure, we cluster the heterogeneous time series of county-level, weekly
220 indoor activity. We find three geographic clusters corresponding to groups of locations that experience
221 similar indoor activity dynamics (Figure 2). These clusters primarily split the country into two clusters: a
222 northern cluster and a southern cluster. Among the communities in the northern cluster, activity is more
223 commonly outdoor over the summer months, trending toward indoor during fall, with a peak in the winter
224 months, as observed in Cook County. Comparatively, the southern cluster has a larger winter peak (i.e.
225 between December and February) and a smaller summer peak (i.e. between July and August); most summer
226 peaks are less extreme than that of Maricopa County (shown). We hypothesize that these two clusters are
227 consistent with climate zones. While there is a moderate association between indoor activity seasonality
228 and environmental variables such as temperature and humidity (Figure 2—figure supplement 2), we expect
229 that the northern and southern indoor activity clusters will be more consistent with climate zones defined
230 for the construction of the indoor built environment and find that there is indeed substantial consistency
231 between the two (Figure 2—figure supplement 3). The third cluster differs substantially: it is geographically
232 discontinuous and its two annual peaks occur during the spring (close to April) and fall (closer to November)
233 seasons. Thus, the counties in this cluster have outdoor activity more frequently than average during both

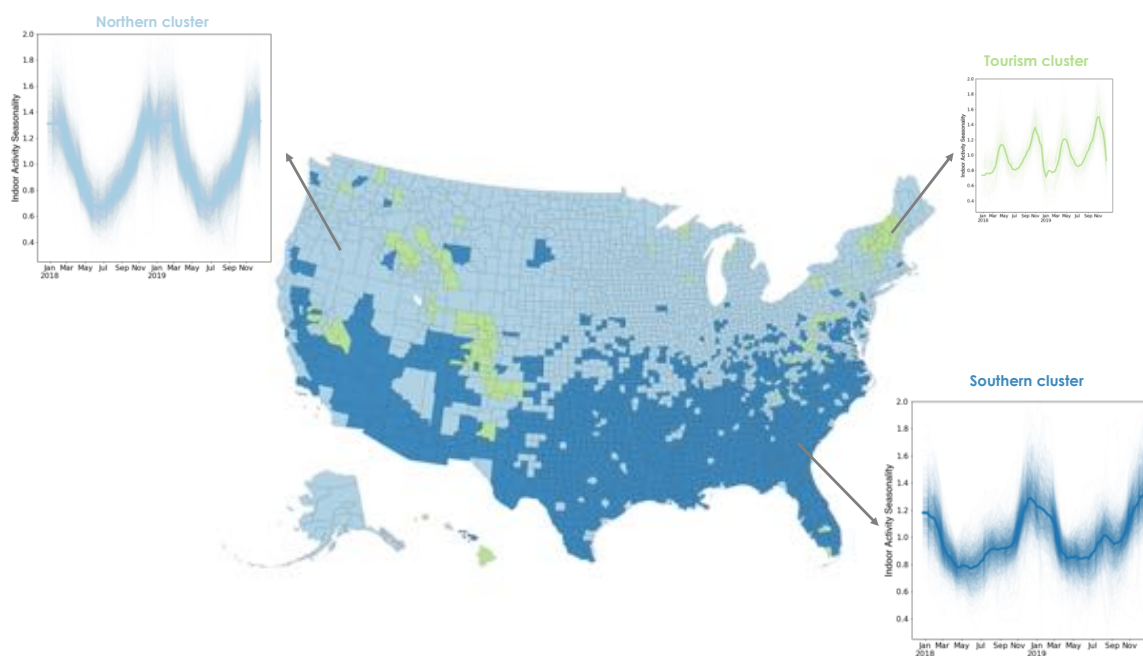


Figure 2: Using a time series clustering approach on the indoor activity time series for each US county, we identify groups of counties that experience similar trends in indoor activity. Locations in the northern cluster (light blue) follow a single peak pattern with the highest indoor activity occurring every winter. Locations in the southern cluster (dark blue) experience two peaks in indoor activity each year, one in the winter and a second, smaller one in the summer. The third cluster also experiences two peaks not matching environmental conditions, but potentially corresponding to winter or other tourism areas. We apply a rolling window mean to the time series for visualization purposes.

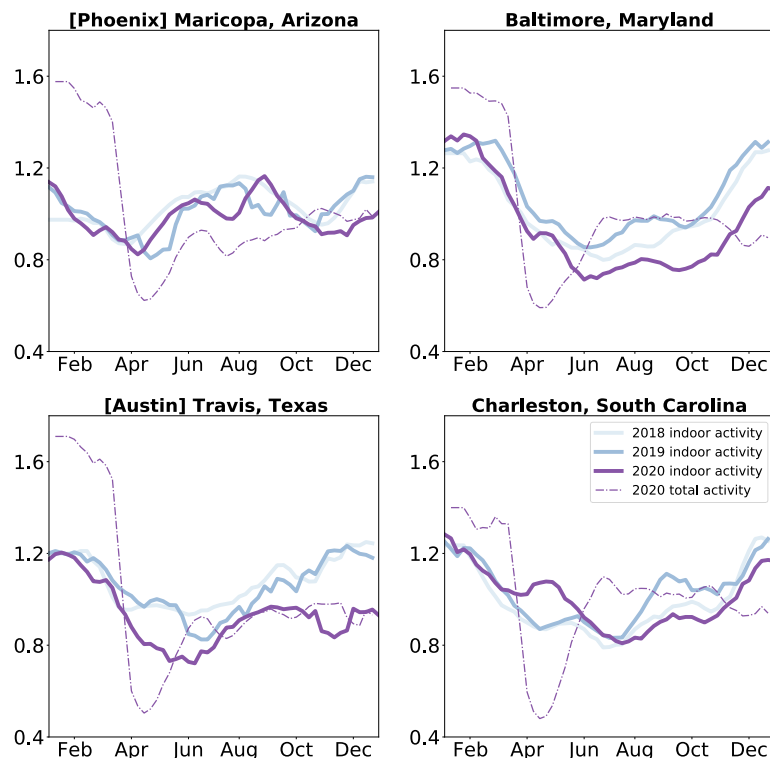


Figure 3: Indoor activity during the COVID-19 pandemic was shifted: We compare indoor activity trends in the baseline years of 2018 and 2019 to the pandemic year 2020 in four case study locations. We find that most locations saw a shift in their indoor activity patterns, while others (such as Maricopa County) did not. We also find that while overall activity was diminished uniformly during the Spring of 2020, indoor activity decreased in some locations (Travis County, Texas and Baltimore County, Maryland) and increased in others (Charleston County, South Carolina). We apply a 3-week rolling window mean to the time series for visualization purposes.

234 the winter and the summer. The counties in this cluster correspond to locations that are hubs for winter or
235 other tourism, which we speculate is driving their unique dynamics (Figure 2—figure supplement 4).

236 Characterizing pandemic disruption to baseline indoor activity seasonality

237 In addition to the description of indoor activity seasonality at baseline, we examine the impact of a large-scale
238 disruption – the COVID-19 pandemic – to these patterns. We compare indoor activity seasonality during the
239 COVID-19 pandemic in 2020 to the baseline patterns of 2018 and 2019. We find that the temporal trends in
240 indoor activity are less geographically structured in 2020 than those of previous years (see Figure 3—figure
241 supplement 2 for a characterization of the time series patterns). We find that indoor activity deviated from
242 pre-pandemic trends beyond interannual deviations (Figure 3—figure supplement 1). We focus on four case
243 studies to highlight the varying impacts on indoor activity of the pandemic disruption (Figure 3). In all four
244 communities, 2020 indoor activity trends shift from 2018 and 2019 patterns, with Maricopa County (home
245 of the city of Phoenix, AZ) showing the least perturbation relative to prior years. We also find that in early

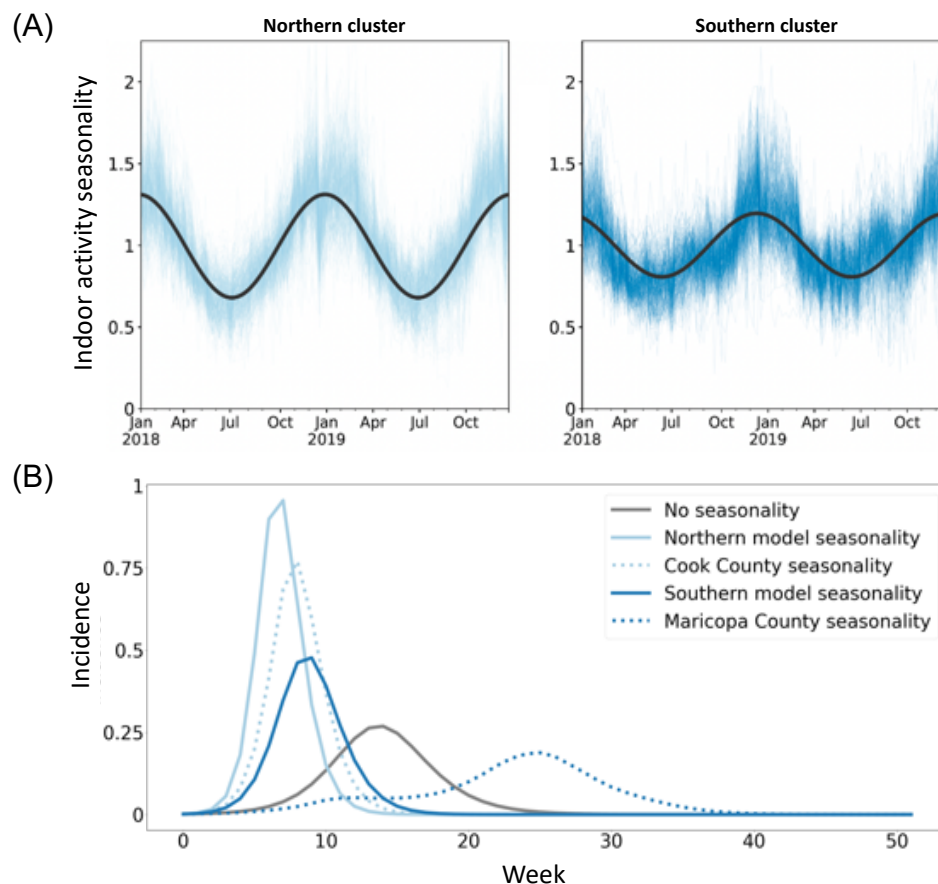


Figure 4: (A) Sine curves fit to the 2018 and 2019 time series data (analogous to seasonal forcing model components) fit the northern cluster better than the southern cluster, with a markedly poorer fit for the southern cluster’s second summer peak. (B) Regional seasonal forcing models display variation in patterns of disease incidence omitted by a non-seasonal model, but even region-level seasonal forcing does not fully capture within-cluster county-level variation.

246 2020, when there was substantial social distancing in the United States (e.g. school closures, remote work),
247 activity was more likely to be outdoor than in prior years, independent of changes in overall activity levels.
248 With our case studies, we highlight that social distancing policies can have different impacts on airborne
249 exposure risk in different locations: while some locations, such as Travis County (home of Austin, Texas),
250 shifted activities outdoors during this period, reducing their overall risk further, other locations, such as
251 Charleston County, South Carolina (home of Charleston, South Carolina) increased indoor activity above
252 the seasonal average during this period, potentially diminishing the effect of reducing overall mobility. The
253 trends in Charleston are representative of those in the southeastern United States during the spring of 2020
254 (Figure 3—figure supplement 1). By the end of 2020 (and the first winter wave of SARS-CoV2), many parts
255 of the country were shifting activity more outdoors than seasonally expected (Figure 3—figure supplement
256 1).

257 Implications for modeling seasonal disease dynamics

258 We use this finely-grained spatiotemporal information on indoor activity to incorporate airborne exposure
259 risk seasonality into compartmental models of disease dynamics using common, coarser seasonal forcing ap-

260 proaches. To investigate the impact of heterogeneity in σ on the estimation of seasonal forcing for infectious
261 disease models, we fit a sinusoidal model to the time series of indoor activity for each of the primary clusters
262 (Figure 4—figure supplement 4A). We note that because σ is defined as deviation from baseline indoor
263 activity, the sinusoidal parameters (amplitude, frequency, phase) should be interpreted as a measure of sea-
264 sonality in indoor activity, relative to each location’s baseline. We find that the parameters of seasonality
265 vary across clusters: the amplitude is higher, and the phase is lower in the northern cluster compared to the
266 southern cluster, indicating a difference in the variability of indoor and outdoor activity seasonality in each
267 cluster (Figure 4—figure supplement 1). While the fits are comparable for both clusters (Figure 4—figure
268 supplement 2), the sinusoidal model does not capture the second peak of indoor activity during the summer
269 months in the southern cluster. These differences in best fit indicate that sinusoidal models may have an
270 overly restrictive functional form, limiting the accuracy of the approximation, and may underestimate the
271 impacts of seasonality on transmission, obscuring systemic differences between regions. Furthermore, differ-
272 ences in seasonal activity of the observed magnitude can have important implications for disease modeling;
273 applying region-level and county-level forcing to a simple disease model alters incidence patterns (figure 4—
274 figure supplement 4B). Although region-level seasonality changes incidence timing and peak size relative to
275 a non-seasonal model, it does not fully capture the changes produced by county-level seasonality. These
276 differences indicate that while coarser geographic approximations of seasonality can be appropriate, these
277 approximations can also oversimplify, reducing the accuracy of disease models. Additionally, while simple
278 models of baseline indoor activity can capture seasonality in exposure risk, disruptions such as pandemics
279 can alter this baseline structure and increase heterogeneity.

280 Discussion

281 The seasonality of influenza, SARS-CoV-2, and other respiratory pathogens depends not only on environ-
282 mental variables but also on the social behavior of hosts. In settings with little prior immunity – such as a
283 pandemic – host social behavior (generating contacts during which transmission may occur) primarily drives
284 heterogeneity in disease dynamics, and seasonality is dwarfed by susceptibility [39]. In settings with higher
285 rates of immunity, contact remains critically important, and seasonal changes in contacts (both direct and
286 indirect) can contribute to the movement of R_t above and below 1 – providing noticeable changes in inci-
287 dence. Although environmental variables play a role in the seasonality of respiratory pathogens, the role of
288 host social behavior in pathogen seasonality is poorly understood, driven by a poor understanding of indoor
289 versus outdoor social interactions and interactions between behavior and the environment. In this study, we
290 propose a fine-grain measure of indoor activity seasonality across time and space. This metric is a relative
291 quantity of behavior, comparable across locations, and thus intended to be a measure of seasonality beyond
292 a baseline. We determine that indoor activity seasonality displays significant spatiotemporal heterogeneity
293 and that this variability is highly geographically structured. We also find that while indoor activity season-
294 ality may be highly predictable under baseline conditions, disruptions such as the COVID-19 pandemic can
295 alter these patterns. Finally, we provide an illustration of how our findings can be incorporated into classical
296 infectious disease models using parsimonious models of exposure seasonality.

297 The indoor activity seasonality that we quantify may reflect heterogeneity in transmission risk via a number
298 of mechanisms including those affecting host contact, susceptibility, or transmissibility. Increased indoor
299 activity may indicate longer-duration airborne contact (e.g., co-location without direct interaction) between
300 susceptible and infected individuals, elevating respiratory transmission risk. Increased indoor density may
301 also suggest increased droplet contact (e.g., a conversation in close proximity), under homogeneous mixing.
302 Additionally, indoor activity may suggest increased susceptibility as poor ventilation, increased pollutants,
303 reduced solar exposure, and low humidity of the indoor environment have been shown to weaken immune
304 response [40]. Finally, increased indoor activity may indicate an increase in transmissibility due to higher
305 exposure as low humidity caused by climate control (heating, ventilation, and cooling, HVAC) in indoor
306 environments has been shown to increase viral survival and HVAC re-circulation has been shown to increase
307 viral dispersion [41, 42]. While our new measure does not disentangle these component mechanisms, it
308 represents an integrated seasonality in exposure risk due to all of these factors and can help lead us to a
309 more complete understanding of the heterogeneity and seasonality in disease dynamics and outcomes.

310 We find that spatiotemporal heterogeneity in the indoor activity metric can be decomposed into two large
311 geographically-contiguous groups in the northern and southern United States representing distinct temporal
312 dynamics in indoor activity. These groups closely correspond to built environment climate zones, potentially
313 explaining this systematic variability. We note, however, that while these clusters overlap with climate
314 classifications, this correspondence does not suggest that environmental variables such as temperature and
315 humidity should be used to represent behavioral heterogeneity. Climatic factors within these climate zones
316 may be related to, but not necessarily correlated with, the seasonality of human mixing within these zones.
317 Additionally, even in the case that environmental factor variability drives behavioral variability, it would be
318 critical to capture the effect of behavior on disease directly so as to not obscure any direct effects of climatic
319 factors on disease.

320 We illustrate how to incorporate seasonality in exposure risk to future models of disease dynamics using a
321 simple phenomenological model. We use this traditional model of infectious disease dynamics to evaluate
322 the implications of the spatial coarseness of seasonal forcing. Our results suggest that the substantial
323 local heterogeneity in the dynamics of indoor activity across time and space could be large enough to alter
324 seasonality in infectious disease dynamics. While our work does not consider observed transmission patterns,
325 we suggest that researchers carefully consider the spatial scale on which they model seasonality in theoretical
326 models, commonly used for scenario analysis and model-based intervention design (e.g., [43]). We additionally
327 highlight that the use of simple or complex functional forms of seasonality requires statistical fits to baseline
328 data, and in the case of disruptions, these fitted models may no longer be appropriate. Although indoor
329 activity is moderately anticorrelated with temperature and humidity (Figure 1). Consequently, weather-
330 derived covariates may have some statistical power to reflect impacts of human movement, but is not able to
331 completely reflect this phenomenon. As we show, patterns of human mobility changed substantially during
332 the COVID-19 pandemic, potentially contributing to changes in infectious disease seasonality.

333 Recent work during the COVID-19 pandemic demonstrates the impact of reduced occupancy in indoor lo-
334 cations and increasing outdoor activity on the likelihood of disease transmission. In particular, behavioral
335 interventions or nudges that reduce occupancy are more impactful than reducing overall mobility as they
336 reduce visitor density and the likelihood of density-dependent airborne transmission [44]. Similarly, the
337 availability of outdoor areas in urban settings, such as public parks, has been demonstrated to reduce case
338 rates when population mobility becomes less restricted [45]. Our results suggest that such public health
339 strategies should be implemented in a targeted manner, informed by real-time data and with clear commu-
340 nication of the goals. We found notable changes occurred in indoor activity seasonality at the start of the
341 COVID-19 pandemic, despite relatively consistent patterns during the spring season in prior years. Designing
342 a behavioral strategy and measuring its effectiveness without real-time data could thus be misleading. Our
343 finding of two distinct geographic clusters of indoor activity suggests the need for geographical targeting of
344 strategies to reduce indoor transmission risk. While northern latitudes might benefit from decreased indoor
345 occupancy and increased outdoor activity in Northern Hemisphere winters, southern latitudes should be
346 additionally targeted for such interventions in the summer months. Lastly, our findings highlight the need to
347 communicate the goals of behavioral interventions clearly. While all communities universally reduced overall
348 activity during the early days of the COVID-19 pandemic, some increased indoor activity during this time,
349 potentially diminishing the positive effects of the social distancing policies put into place. A public health
350 education campaign to clarify the role of indoor interactions in transmission risk may have ameliorated this.

351 Our study leverages a novel data stream made available to researchers due to the COVID-19 pandemic.
352 Similar datasets are available globally, part of a \$12 billion location intelligence industry [46]. Such novel
353 data streams offer many opportunities to address long-unanswered questions in infectious disease and climate
354 change behavior dynamics, but these data must be interpreted carefully. Safegraph's mobile-app-based
355 location data does not include data on individuals less than 16 years of age [47]. While we may expect that
356 children under 12 may be accompanied by adults that may be represented in the dataset, our metric likely
357 does not capture the activity dynamics of older children (children 12-15 make up 5% of the US population).
358 For those included in the Safegraph database, representation is dependent on smartphone usage and a number
359 of business processes not transparent to users of the data, thus we expect that there is geographic variation
360 in the representativeness of the data. Smartphone ownership has increased in recent years, with 85% of US
361 adults reporting smartphone ownership; however, smartphone usage does vary significantly by age, with only
362 61% of adults over 65 reporting smartphone use [48]. Additionally, data shows that location sharing among

363 mobile users is not significantly biased by age, gender, race/ethnicity, income, or education (with 40-65%
364 of all demographic groups participating in location sharing) [49]. Based on an analysis done by Safegraph,
365 the panel is representative of race, educational attainment, and income [50]. On the other hand, a recent
366 independent analysis shows that older and non-white individuals are less likely to be captured in the panel
367 for POI-specific analyses [51]. It is important to note that both studies are associative in nature as the
368 devices in the panel are fully anonymized, so no device-level demographic data exists. Continued work to
369 understand the sampling biases of such datasets will be needed so that improved bias correction approaches
370 can be developed [51]. Additionally, we limit our scope in this study to consider only the number of visits
371 and do not incorporate information about visit duration. The dataset counts all visits of one minute or
372 longer. For disease transmission, there may be a threshold duration required for an interaction between an
373 infected and susceptible individual for infection to be propagated. These thresholds are not well-understood
374 for all respiratory diseases, but evidence that SARS-CoV-2 transmission can occur with brief encounters has
375 emerged [52]. While the Safegraph dataset does provide median dwell times for POIs, the likely significant
376 heterogeneity in the distribution of dwell times remains unknown and is difficult to capture in an aggregated
377 manner.

378 Our metric and analysis also focus on the US county scale to reflect the finest scale generally used for
379 infectious disease modeling as well as public health decision-making. This choice is likely to ignore some
380 within-county heterogeneity and means that our metric does not represent the experience of all groups,
381 particularly by socioeconomic status. For example, low-income and racially marginalized communities have
382 systematically less access to outdoor, natural spaces and spend more time indoors due to structural inequities
383 including lack of paid leave [28, 53, 54]. Such socio-economic disparities have been further exacerbated during
384 the pandemic, which potentially affects our indoor activity estimates during 2021. Thus, our estimate of a
385 county's indoor transmission risk may represent an underestimate of the risk experienced by individuals in
386 these communities. We commit to continued work to better characterize the transmission risk experienced
387 by vulnerable populations. Lastly, we acknowledge that data modeling work that can influence public health
388 policy decisions, particularly during an ongoing crisis, must be done with care to prevent misconceptions
389 from having adverse effects on risk perception and policies [55]. We thus strongly note that while our measure
390 of indoor behavioral seasonality provides a potential driver of respiratory disease seasonality, it remains one
391 among many complex factors which integrate to predict the transmission potential of an ongoing epidemic
392 or pandemic [56]. Thus we cannot rely on behavioral seasonality to diminish transmission naturally, and
393 pandemic intervention strategies should not be planned around behavioral seasonality while population
394 susceptibility remains high in so many locations.

395 Ongoing global change events highlight the importance of this work, as it informs how widespread interrup-
396 tions may shift patterns of indoor activity, potentially altering traditional infectious disease seasonality.
397 Climate change events will continue to cause significant disruption to normal behavior patterns; mechanistic
398 understanding of infectious disease seasonality and real-time data collection will be crucial components of
399 future disease control efforts. While other global change events may impact indoor activity in different ways
400 than the COVID-19 pandemic, a rigorous understanding of the impact of host behavior on infectious disease
401 allows policymakers and emergency preparedness experts to effectively address future disruptions.

402 Data Availability

403 We make available on Github the data and code needed to reproduce all figures and analyses in this
404 manuscript: https://github.com/bansallab/indoor_outdoor. This dataset is of the metric used in all
405 our analyses and figures (“indoor activity”). This dataset can be regenerated using the Safegraph Patterns
406 and Places datasets found at <https://www.safegraph.com/covid-19-data-consortium> and code in the

407 Github repository.

408 Competing Interests

409 The authors declare that they have no competing interests.

410 Acknowledgments

411 Research reported in this publication was supported by the National Institute of General Medical Sciences of
412 the National Institutes of Health under award number R01GM123007. The content is solely the responsibility
413 of the authors and does not necessarily represent the official views of the National Institutes of Health.

414 We gratefully acknowledge data sharing by Safegraph which made this study possible. We thank Alexes
415 Merritt for her data processing efforts.

416 References

- 417 [1] Micaela Elvira Martinez. The calendar of epidemics: Seasonal cycles of infectious diseases. *PLoS*
418 *Pathogens*, 14(11):e1007327, 2018.
- 419 [2] Sonia Altizer, Andrew Dobson, Parvize Hosseini, Peter Hudson, Mercedes Pascual, and Pejman Rohani.
420 Seasonality and the dynamics of infectious diseases. *Ecology Letters*, 9(4):467–484, 2006.
- 421 [3] Nicholas C Grassly and Christophe Fraser. Seasonal infectious disease epidemiology. *Proceedings of the*
422 *Royal Society B: Biological Sciences*, 273(1600):2541–2550, 2006.
- 423 [4] Jeffrey Shaman and Melvin Kohn. Absolute humidity modulates influenza survival, transmission, and
424 seasonality. *Proceedings of the National Academy of Sciences*, 106(9):3243–3248, 2009.
- 425 [5] Jeffrey Shaman, Virginia E Pitzer, Cécile Viboud, Bryan T Grenfell, and Marc Lipsitch. Absolute hu-
426 midity and the seasonal onset of influenza in the continental United States. *PLoS Biology*, 8(2):e1000316,
427 2010.
- 428 [6] Benjamin D Dalziel, Stephen Kissler, Julia R Gog, Cecile Viboud, Ottar N Bjørnstad, C Jessica E
429 Metcalf, and Bryan T Grenfell. Urbanization and humidity shape the intensity of influenza epidemics
430 in US cities. *Science*, 362(6410):75–79, 2018.
- 431 [7] Rachel E Baker, Ayesha S Mahmud, Caroline E Wagner, Wenchang Yang, Virginia E Pitzer, Cecile
432 Viboud, Gabriel A Vecchi, C Jessica E Metcalf, and Bryan T Grenfell. Epidemic dynamics of respiratory
433 syncytial virus in current and future climates. *Nature Communications*, 10(1):1–8, 2019.
- 434 [8] Daisuke Onozuka and Masahiro Hashizume. The influence of temperature and humidity on the incidence
435 of hand, foot, and mouth disease in Japan. *Science of the Total Environment*, 410:119–125, 2011.
- 436 [9] C Jessica E Metcalf, Ottar N Bjørnstad, Bryan T Grenfell, and Viggo Andreasen. Seasonality and
437 comparative dynamics of six childhood infections in pre-vaccination Copenhagen. *Proceedings of the*
438 *Royal Society B: Biological Sciences*, 276(1676):4111–4118, 2009.
- 439 [10] Joël Mossong, Niel Hens, Mark Jit, Philippe Beutels, Kari Auranen, Rafael Mikolajczyk, Marco Massari,
440 Stefania Salmaso, Gianpaolo Scalia Tomba, Jacco Wallinga, et al. Social contacts and mixing patterns
441 relevant to the spread of infectious diseases. *PLoS Medicine*, 5(3):e74, 2008.
- 442 [11] Noga Kronfeld-Schor, Tamara J Stevenson, Sema Nickbakhsh, Eva S Schernhammer, Xaquín C Dopico,
443 Tamar Dayan, Maria Martinez, and Barbara Helm. Drivers of infectious disease seasonality: potential
444 implications for COVID-19. *Journal of Biological Rhythms*, 36(1):35–54, 2021.

- 445 [12] Kevin M Bakker, Marisa C Eisenberg, Robert Woods, and Micaela E Martinez. Exploring the seasonal
446 drivers of varicella zoster transmission and reactivation. *American Journal of Epidemiology*, 2021.
- 447 [13] D Fisman. Seasonality of viral infections: mechanisms and unknowns. *Clinical Microbiology and Infec-*
448 *tion*, 18(10):946–954, 2012.
- 449 [14] Nita Bharti, Andrew J Tatem, Matthew J Ferrari, Rebecca F Grais, Ali Djibo, and Bryan T Gren-
450 fell. Explaining seasonal fluctuations of measles in Niger using nighttime lights imagery. *Science*,
451 334(6061):1424–1427, 2011.
- 452 [15] Roger Few, Iain Lake, Paul R Hunter, and Pham Gia Tran. Seasonality, disease and behavior: Using
453 multiple methods to explore socio-environmental health risks in the Mekong Delta. *Social Science &*
454 *Medicine*, 80:1–9, 2013.
- 455 [16] Allisandra G Kummer, Juanjuan Zhang, Maria Litvinova, Alessandro Vespignani, Hongjie Yu, and
456 Marco Ajelli. Measuring the seasonality of human contact patterns and its implications for the spread
457 of respiratory infectious diseases. *medRxiv*, 2022.
- 458 [17] Raymond Tellier, Yuguo Li, Benjamin J Cowling, and Julian W Tang. Recognition of aerosol transmis-
459 sion of infectious agents: a commentary. *BMC infectious diseases*, 19(1):1–9, 2019.
- 460 [18] Trisha Greenhalgh, Jose L Jimenez, Kimberly A Prather, Zeynep Tufekci, David Fisman, and Robert
461 Schooley. Ten scientific reasons in support of airborne transmission of SARS-CoV-2. *The Lancet*,
462 397(10285):1603–1605, 2021.
- 463 [19] Chia C Wang, Kimberly A Prather, Josué Sznitman, Jose L Jimenez, Seema S Lakdawala, Zeynep
464 Tufekci, and Linsey C Marr. Airborne transmission of respiratory viruses. *Science*, 373(6558):eabd9149,
465 2021.
- 466 [20] Mahesh Jayaweera, Hasini Perera, Buddhika Gunawardana, and Jagath Manatunge. Transmission of
467 COVID-19 virus by droplets and aerosols: A critical review on the unresolved dichotomy. *Environmental*
468 *Research*, 188:109819, 2020.
- 469 [21] Michael Klompas, Meghan A Baker, and Chanu Rhee. Airborne transmission of SARS-CoV-2: theoret-
470 ical considerations and available evidence. *JAMA*, 2020.
- 471 [22] Lidia Morawska and Donald K Milton. It is time to address airborne transmission of coronavirus disease
472 2019 (COVID-19). *Clinical Infectious Diseases*, 71(9):2311–2313, 2020.
- 473 [23] Jennifer L Nguyen and Douglas W Dockery. Daily indoor-to-outdoor temperature and humidity rela-
474 tionships: a sample across seasons and diverse climatic regions. *International Journal of Biometeorology*,
475 60(2):221–229, 2016.
- 476 [24] Alison J Robey and Laura Fierce. Sensitivity of airborne transmission of enveloped viruses to sea-
477 sonal variation in indoor relative humidity. *International Communications in Heat and Mass Transfer*,
478 130:105747, 2022.
- 479 [25] Wan Yang and Linsey C Marr. Dynamics of airborne influenza A viruses indoors and dependence on
480 humidity. *PloS one*, 6(6):e21481, 2011.
- 481 [26] Wayne R Ott. *Human activity patterns: a review of the literature for estimating time spent indoors,*
482 *outdoors, and in transit*. US Environmental Protection Agency, 1988.
- 483 [27] Neil E Klepeis, William C Nelson, Wayne R Ott, John P Robinson, Andy M Tsang, Paul Switzer,
484 Joseph V Behar, Stephen C Hern, and William H Engelmann. The National Human Activity Pattern
485 Survey (NHAPS): a resource for assessing exposure to environmental pollutants. *Journal of Exposure*
486 *Science & Environmental Epidemiology*, 11(3):231–252, 2001.

- 487 [28] Elizabeth W Spalt, Cynthia L Curl, Ryan W Allen, Martin Cohen, Sara D Adar, Karen H Stukovsky,
488 Ed Avol, Cecilia Castro-Diehl, Cathy Nunn, Karen Mancera-Cuevas, et al. Time–location patterns of a
489 diverse population of older adults: the Multi-Ethnic Study of Atherosclerosis and Air Pollution (MESA
490 Air). *Journal of exposure science & environmental epidemiology*, 26(4):349–355, 2016.
- 491 [29] Pietro Coletti, Chiara Poletto, Clément Turbelin, Thierry Blanchon, and Vittoria Colizza. Shifting
492 patterns of seasonal influenza epidemics. *Scientific Reports*, 8(1):1–12, 2018.
- 493 [30] Matt J Keeling, Pejman Rohani, and Bryan T Grenfell. Seasonally forced disease dynamics explored as
494 switching between attractors. *Physica D: Nonlinear Phenomena*, 148(3-4):317–335, 2001.
- 495 [31] Safegraph. Safegraph Patterns. <https://safegraph.com/>, 2021 (Last accessed February 14, 2022).
- 496 [32] Statista Digital Market Outlook. Individuals of any age who own at least one smartphone and
497 use the smartphone(s) at least once per month. [https://www.statista.com/statistics/201182/
498 forecast-of-smartphone-users-in-the-us/](https://www.statista.com/statistics/201182/forecast-of-smartphone-users-in-the-us/), 2022 (Last accessed Feb 17, 2022).
- 499 [33] Charu C. Aggarwal and Chandan K. Reddy. *Data Clustering: Algorithms and Applications*. Chapman
500 & Hall/CRC, 1st edition, 2013.
- 501 [34] Vincent D Blondel, Jean-Loup Guillaume, Renaud Lambiotte, and Etienne Lefebvre. Fast unfold-
502 ing of communities in large networks. *Journal of Statistical Mechanics: Theory and Experiment*,
503 2008(10):P10008, 2008.
- 504 [35] Vincent Traag. Louvain-igraph. [https://louvain-igraph.readthedocs.io/en/latest/reference.
505 html](https://louvain-igraph.readthedocs.io/en/latest/reference.html), 2018 (Last accessed Feb 17, 2019).
- 506 [36] Till Hoffmann, Leto Peel, Renaud Lambiotte, and Nick S Jones. Community detection in networks
507 without observing edges. *Science advances*, 6(4):eaav1478, 2020.
- 508 [37] Michael R Berthold and Frank Höppner. On clustering time series using euclidean distance and pearson
509 correlation. *arXiv preprint arXiv:1601.02213*, 2016.
- 510 [38] Brennan Klein, Timothy LaRock, Stefan McCabe, Leo Torres, Lisa Friedland, Maciej Kos, Filippo
511 Privitera, Brennan Lake, Moritz UG Kraemer, John S Brownstein, et al. Characterizing collective
512 physical distancing in the us during the first nine months of the covid-19 pandemic. *arXiv preprint
513 arXiv:2212.08873*, 2022.
- 514 [39] Rachel E Baker, Wenchang Yang, Gabriel A Vecchi, C Jessica E Metcalf, and Bryan T Grenfell. Suscep-
515 tible supply limits the role of climate in the early SARS-CoV-2 pandemic. *Science*, 369(6501):315–319,
516 2020.
- 517 [40] Miyu Moriyama, Walter J Hugentobler, and Akiko Iwasaki. Seasonality of respiratory viral infections.
518 *Annual review of virology*, 7:83–101, 2020.
- 519 [41] Jianyun Lu, Jieni Gu, Kuibiao Li, Conghui Xu, Wenzhe Su, Zhisheng Lai, Deqian Zhou, Chao Yu, Bin
520 Xu, and Zhicong Yang. COVID-19 outbreak associated with air conditioning in restaurant, Guangzhou,
521 China, 2020. *Emerging infectious diseases*, 26(7):1628, 2020.
- 522 [42] Chung-Min Liao, Chao-Fang Chang, and Huang-Min Liang. A probabilistic transmission dynamic
523 model to assess indoor airborne infection risks. *Risk Analysis: An International Journal*, 25(5):1097–
524 1107, 2005.
- 525 [43] Rebecca K Borchering, Cécile Viboud, Emily Howerton, Claire P Smith, Shaun Truelove, Michael C
526 Runge, Nicholas G Reich, Lucie Contamin, John Levander, Jessica Salerno, et al. Modeling of future
527 covid-19 cases, hospitalizations, and deaths, by vaccination rates and nonpharmaceutical intervention
528 scenarios—united states, april–september 2021. *Morbidity and Mortality Weekly Report*, 70(19):719,
529 2021.

- 530 [44] Serina Chang, Emma Pierson, Pang Wei Koh, Jaline Gerardin, Beth Redbird, David Grusky, and Jure
531 Leskovec. Mobility network models of COVID-19 explain inequities and inform reopening. *Nature*,
532 589(7840):82–87, 2021.
- 533 [45] Thomas F Johnson, Lisbeth A Hordley, Matthew P Greenwell, and Luke C Evans. Associations between
534 COVID-19 transmission rates, park use, and landscape structure. *Science of the Total Environment*,
535 789:148123, 2021.
- 536 [46] Jon Keegan and Alfred Ng. There’s a multibillion-dollar market for your phone’s location data. *The*
537 *Markup*, 2021.
- 538 [47] Safegraph. Privacy Policy. <https://www.safegraph.com/privacy-policy>, 2021 (Last accessed Feb
539 17, 2022).
- 540 [48] Pew Resesarch Center. Mobile Fact Sheet. [https://www.pewresearch.org/internet/fact-sheet/
541 mobile/](https://www.pewresearch.org/internet/fact-sheet/mobile/), 2021 (Last accessed Feb 17, 2022).
- 542 [49] Kathryn Zickuhr and Aaron Smith. 28% of american adults use mobile and social location-based services.
543 2011.
- 544 [50] Ryan Fox. "What about bias in your dataset?": Quantifying Sampling Bias in SafeGraph Patterns.
545 <https://colab.research.google.com/drive/1u15afRytJMsizySFqA2EP1XSh3KTmNTQ>, 2019 (Last ac-
546 cessed Feb 17, 2022).
- 547 [51] Amanda Coston, Neel Guha, Derek Ouyang, Lisa Lu, Alexandra Chouldechova, and Daniel E Ho.
548 Leveraging administrative data for bias audits: Assessing disparate coverage with mobility data for
549 COVID-19 policy. In *Proceedings of the 2021 ACM Conference on Fairness, Accountability, and Trans-*
550 *parency*, pages 173–184, 2021.
- 551 [52] Julia C Pringle, Jillian Leikauskas, Sue Ransom-Kelley, Benjamin Webster, Samuel Santos, Heidi Fox,
552 Shannon Marcoux, Patsy Kelso, and Natalie Kwit. COVID-19 in a correctional facility employee fol-
553 lowing multiple brief exposures to persons with COVID-19—vermont, july–august 2020. *Morbidity and*
554 *Mortality Weekly Report*, 69(43):1569, 2020.
- 555 [53] Lorien Nesbitt, Michael J Meitner, Cynthia Girling, Stephen RJ Sheppard, and Yuhao Lu. Who has
556 access to urban vegetation? a spatial analysis of distributional green equity in 10 US cities. *Landscape*
557 *and Urban Planning*, 181:51–79, 2019.
- 558 [54] Justine S Sefcik, Michelle C Kondo, Heather Klusaritz, Elisa Sarantschin, Sara Solomon, Abbey Roepke,
559 Eugenia C South, and Sara F Jacoby. Perceptions of nature and access to green space in four urban
560 neighborhoods. *International Journal of Environmental Research and Public Health*, 16(13):2313, 2019.
- 561 [55] Colin J Carlson, Ana CR Gomez, Shweta Bansal, and Sadie J Ryan. Misconceptions about weather
562 and seasonality must not misguide COVID-19 response. *Nature Communications*, 11(1):1–4, 2020.
- 563 [56] Zachary Susswein, Eugenio Valdano, Tobias Brett, Pej Rohani, Vittoria Colizza, and Shweta Bansal.
564 Ignoring spatial heterogeneity in drivers of SARS-CoV-2 transmission in the US will impede sustained
565 elimination. *medRxiv*, 2021.
- 566 [57] Fedor Mesinger, Geoff DiMego, Eugenia Kalnay, Kenneth Mitchell, Perry C Shafran, Wesley Ebisuzaki,
567 Dušan Jović, Jack Woollen, Eric Rogers, Ernesto H Berbery, et al. North american regional reanalysis.
568 *Bulletin of the American Meteorological Society*, 87(3):343–360, 2006.
- 569 [58] International Code Council. 2012 International Energy Conservation Code , Printed 2015.

570 Supplementary Figures

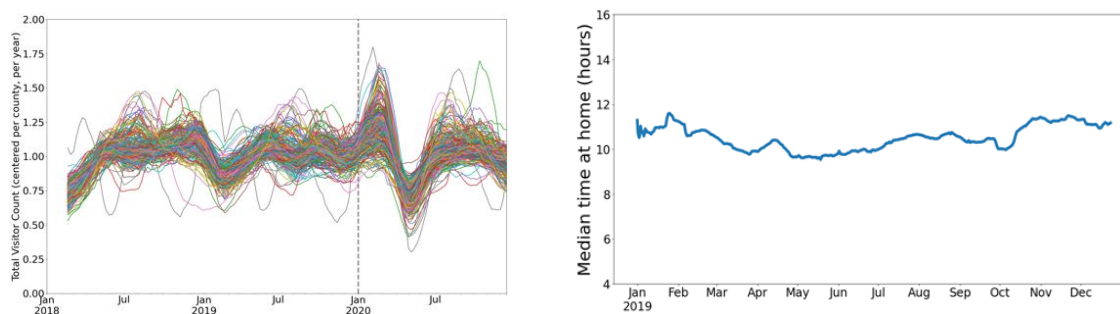


Figure 1—figure supplement 1: Left: Using the Safegraph Weekly Patterns dataset (<https://docs.safegraph.com/docs/weekly-patterns>), we show total (all non-home locations) visitor counts for a random sample of 310 counties (10% of all US counties). Overall mobility does not appear to be highly seasonal. Right: Using the Safegraph Social Distancing Metrics dataset (<https://docs.safegraph.com/docs/social-distancing-metrics>), we show time spent at home for a random sample of 310 counties (10% of all US counties). While home locations are not included in our indoor activity metric, time spent at home does not appear to be highly seasonal.

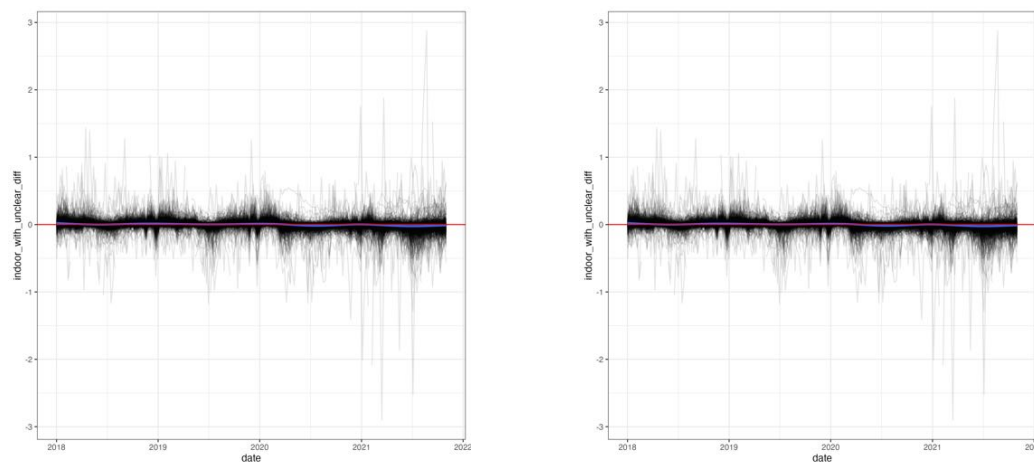


Figure 1—figure supplement 2: We demonstrate the effect of the "unclear" locations on the indoor activity seasonality. In the left panel, we show the difference in σ if all "unclear" locations were to be classified as indoor. In the right panel, we show the difference if σ if all "unclear" locations are classified as outdoor.

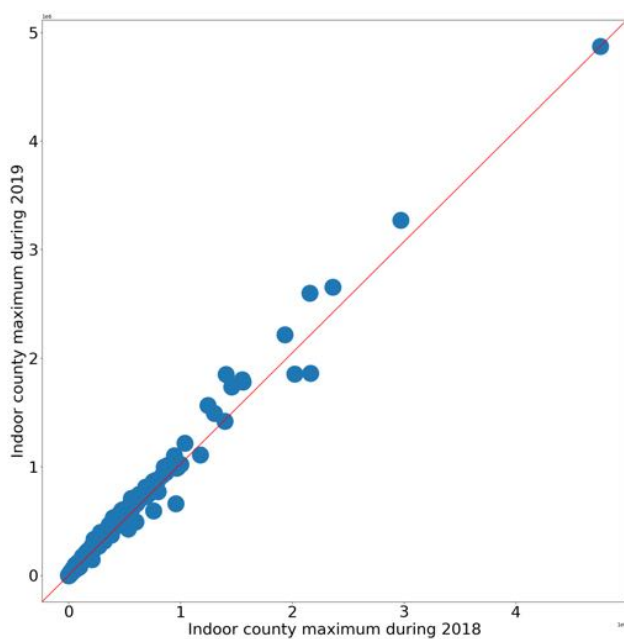
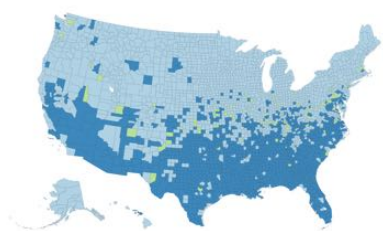
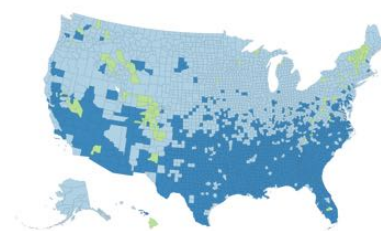


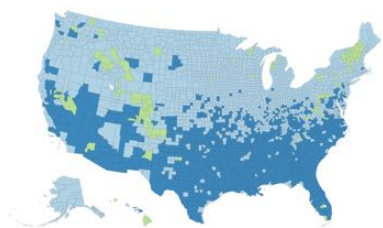
Figure 1—figure supplement 3: We show that the maximum number of visits used in the definition of the σ metric are highly comparable in 2018 and 2019.



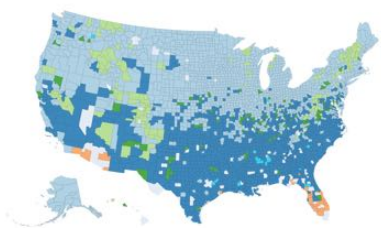
(a) 50th percentile, $\rho > 0.42$, NMI = 0.60



(b) 75th percentile, $\rho > 0.54$, NMI = 0.74



(c) 90th percentile, $\rho > 0.67$



(d) 99th percentile, $\rho > 0.82$, NMI = 0.67

Figure 1—figure supplement 4: We illustrate the impact of the correlation threshold on the clustering results (without post processing). For each panel, we list the percentile for time series correlations used as the threshold, the corresponding correlation value (ρ), and the normalized mutual information between each partition and the partition with the 90th percentile threshold (corresponding to the partition presented in Figure 2).

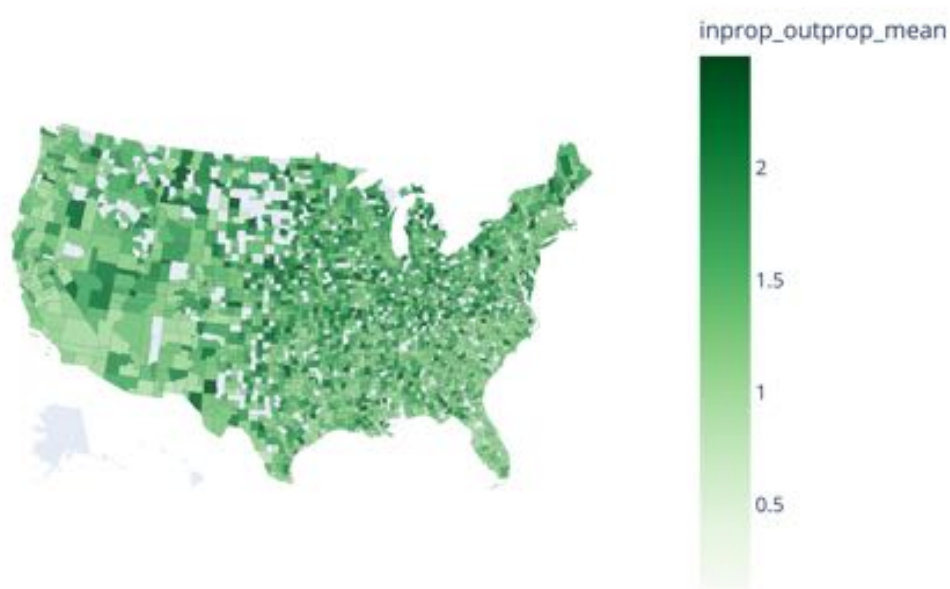


Figure 2—figure supplement 1: The mean proportion of indoor/outdoor activity (μ_{σ}) in 2018 displays no latitudinal gradient and is relatively homogeneous across counties; outliers of mean ≥ 2.5 are removed

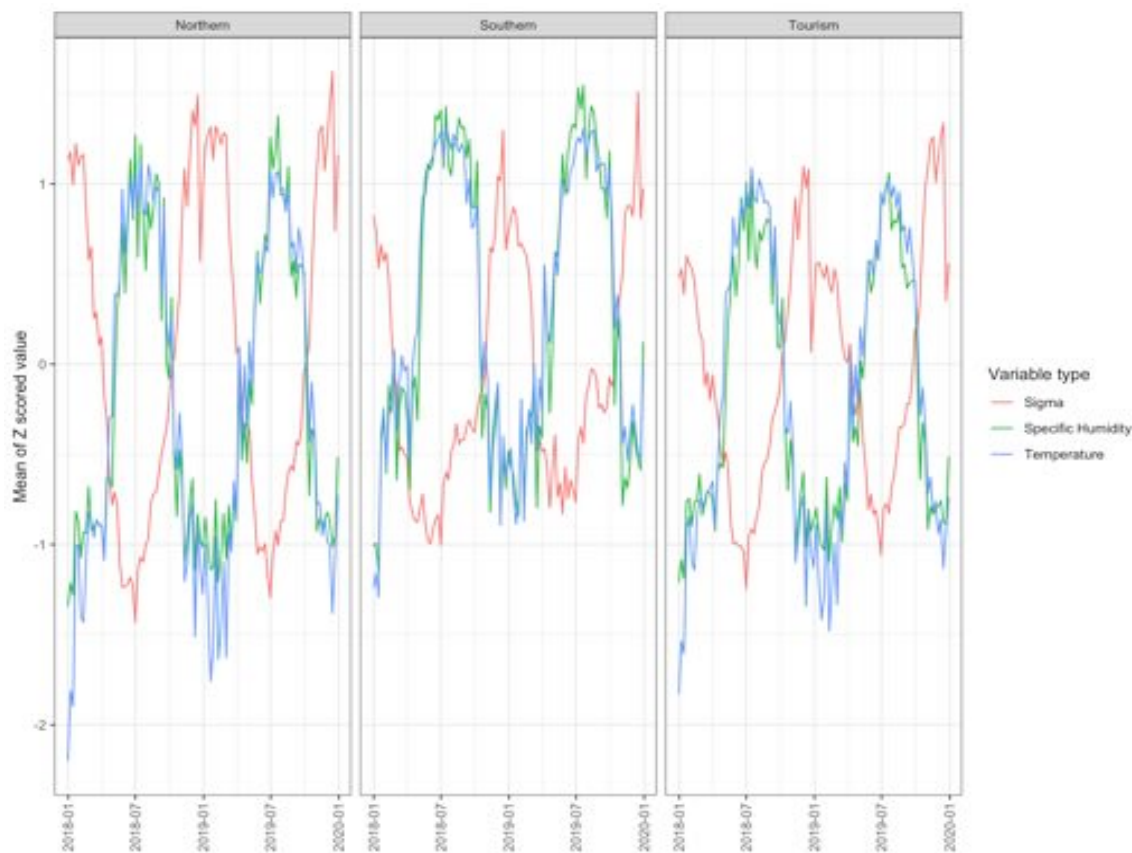


Figure 2—figure supplement 2: Using data on temperature and rainfall from NOAA’s North American Regional Reanalysis [57], we find that indoor activity (sigma) is moderately anticorrelated with both temperature and humidity. Temperature and humidity are strongly correlated in all three clusters (pearson’s $\rho \approx 0.87$). Across the three clusters, indoor activity is moderately associated with temperature ($\rho \approx -0.52$). Likewise, indoor activity is moderately anticorrelated with humidity ($\rho \approx -0.45$).

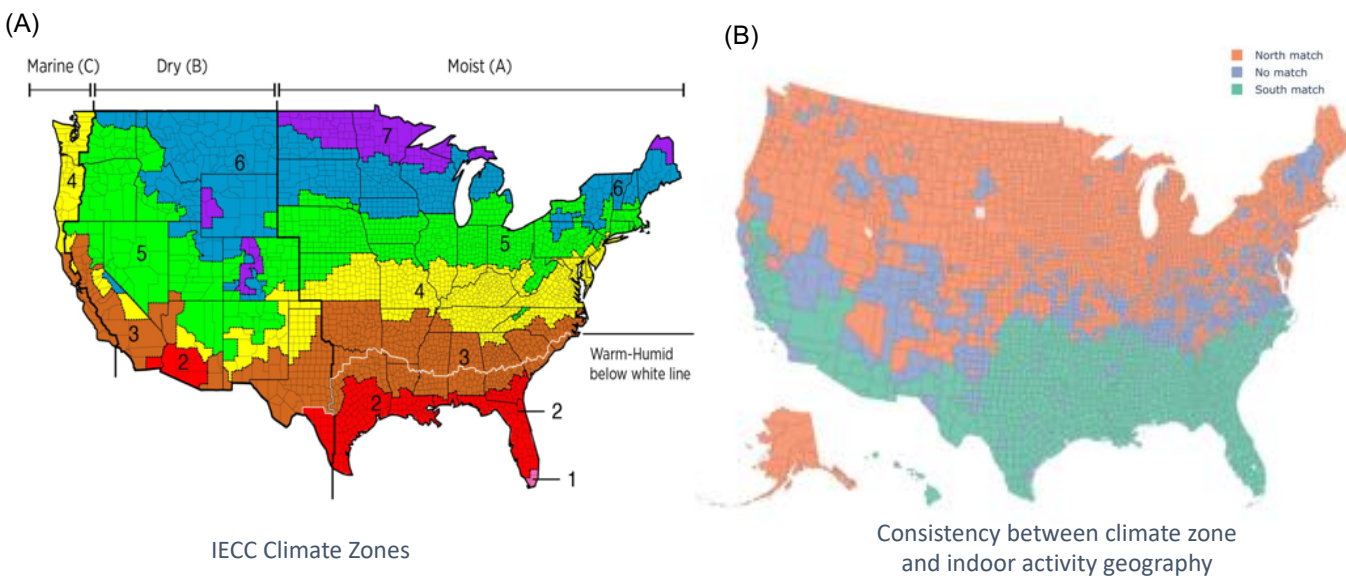


Figure 2—figure supplement 3: (A) The IECC climate zones are based on temperature, humidity, and rainfall in each county and govern the type building material and amount of ventilation required in a building [58]. (B) The consistency between the two primary clusters of indoor activity identified by our analysis and the IECC climate zones. Treating the IECC climate zones as "ground truth", we quantify the ability of our indoor activity clusters to predict the IECC climate zones. We achieve this by collapsing the partitions into two clusters each (the tourism cluster is grouped with the northern cluster in the indoor activity clustering; and IECC climate zones 1/2/3 are grouped into one cluster and zones 4/5/6/7 into another cluster). Our indoor activity clusters have a 0.72 F1-score, with a precision of 0.92 and a recall score of 0.59 with the IECC zones.

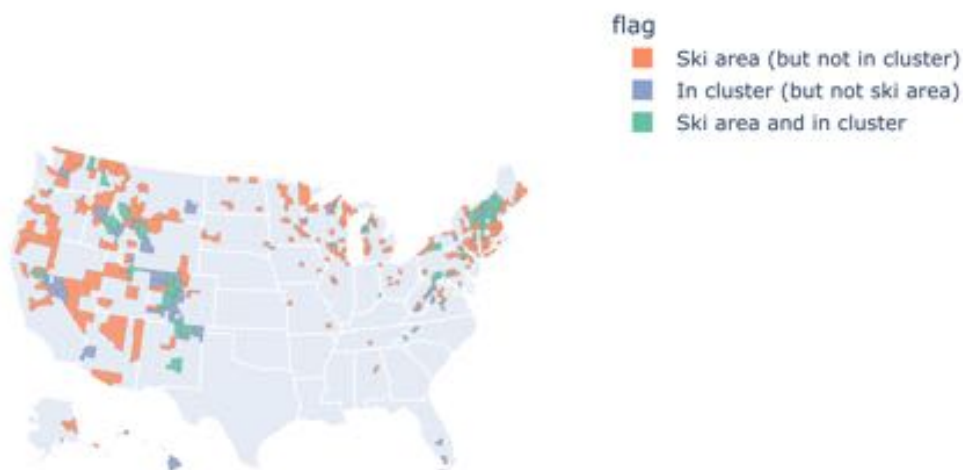


Figure 2—figure supplement 4: The third indoor activity cluster displays some correlation with areas of increased tourism, including US ski areas in western and northeastern states, potentially contributing to off-season activity increases. Most areas in the cluster are either in a ski area or neighbor a ski area, with some parts of Hawaii and Florida being clear outliers of this pattern and suggests other types of tourism lead to similar behavioral seasonality.

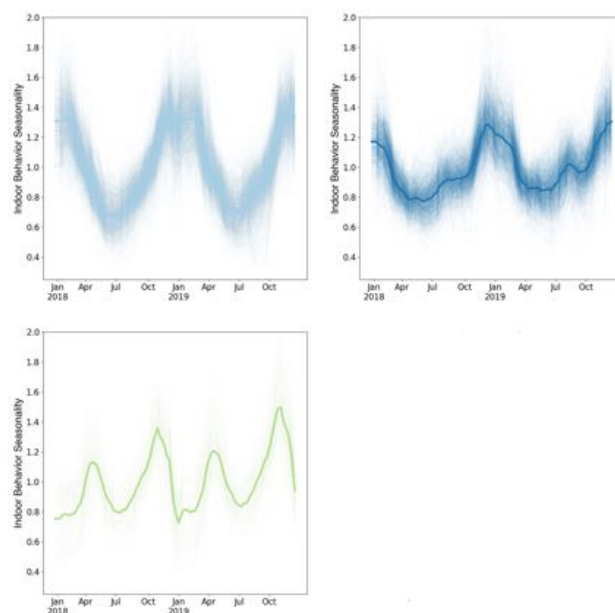
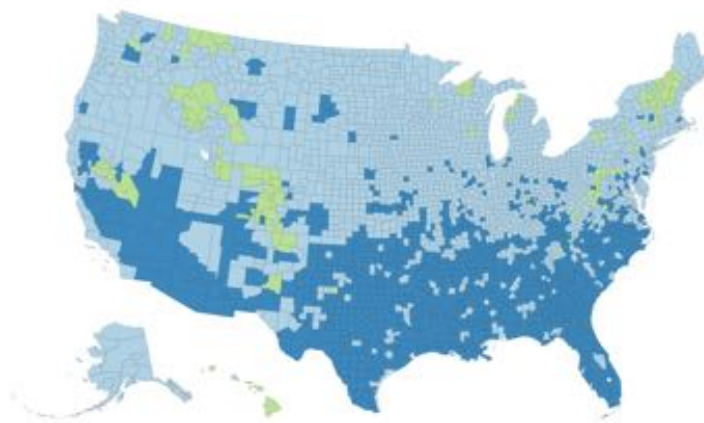
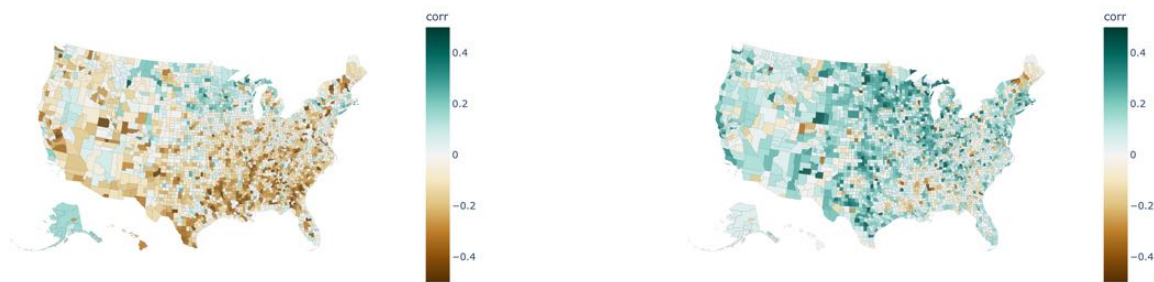


Figure 2—figure supplement 5: We show the results of time series clustering based on a hierarchical clustering method using Ward linkage and Euclidean distance, implemented using `scipy.cluster` in *Python*. This partition has high similarity to the network-based clustering algorithm results we illustrate in Figure 2: normalized mutual information = 0.56 with 89% of counties matching on cluster identity.

	2018/2019	2018/2020	2019/2020
Euclidean distance	1.1	1.5	1.5

(a) Interannual deviations



(b) Deviations during Spring 2020

(c) Deviations during Winter 2020

Figure 3—figure supplement 1: Top: Euclidean distance between indoor activity time series in corresponding years for each county, averaged over all counties. The 2020 time series show a higher deviation from each of the baseline years than the two baseline years do from each other. Bottom: We illustrate the mean difference in indoor activity at baseline (defined as the average of 2018 and 2019) and 2020 for two time periods: (a) Week 10 to Week 20 in spring 2020 during the initial lockdown period for COVID-19. (b) Week 44 to Week 52 in winter 2020 during the first winter surge of COVID-19. Positive mean differences suggest more outdoor activity in 2020 than at baseline and negative mean differences suggest more indoor activity in 2020 than at baseline.

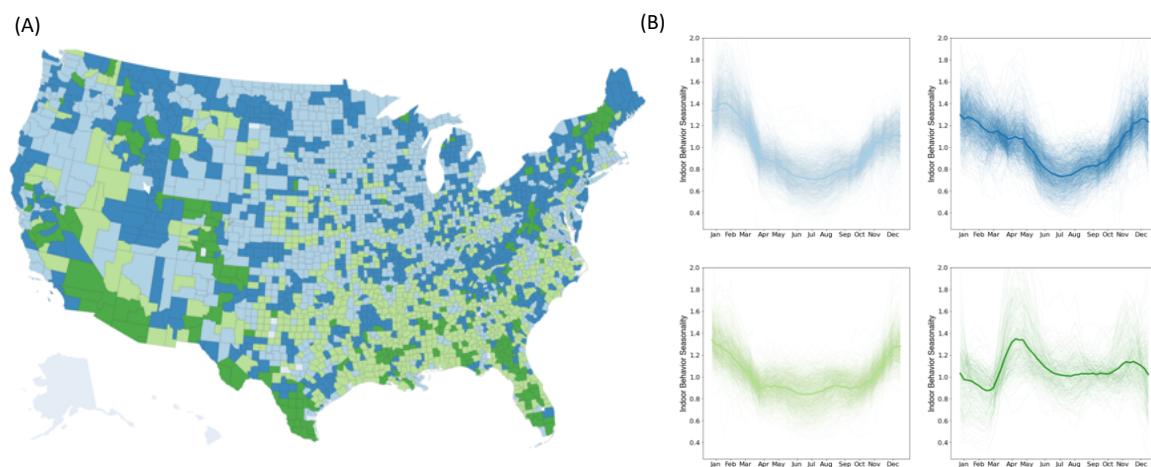
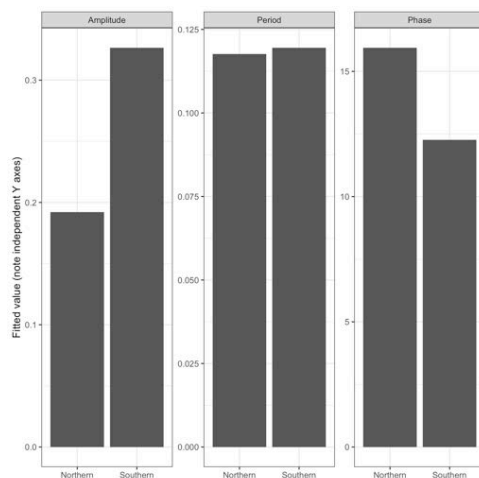


Figure 3—figure supplement 2: (A) Indoor seasonality during 2020 can be clustered into four groups, although clusters are more geographically fragmented than previous years. (B) Time series for 2020 indoor seasonality clusters display heterogeneous trends that were not apparent in previous years, with some clusters more variable than others.



Estimates and cluster differences			
term	Northern	Southern	diff
Amplitude	0.1921964	0.3264692	-0.134272737
Period	0.1176322	0.1195019	-0.001869687
Phase	15.9414221	12.2645018	3.676920333

Figure 4—figure supplement 1: Top: Inferred parameters for the sinusoidal model fits of the indoor activity data for the northern and southern clusters show a similar frequency, but greater amplitude and shorter phase in the southern cluster. Values displayed are mean parameter estimates. Standard errors for all parameters are smaller than $5e-3$ and thus are not displayed. Bottom: We show the estimated parameters for the parameters of the sine curve fits to the Northern and Southern clusters as well as the difference between the parameter estimates. The period is in units of time (weeks). The amplitude matches the units of σ . The phase is in units of time (weeks).

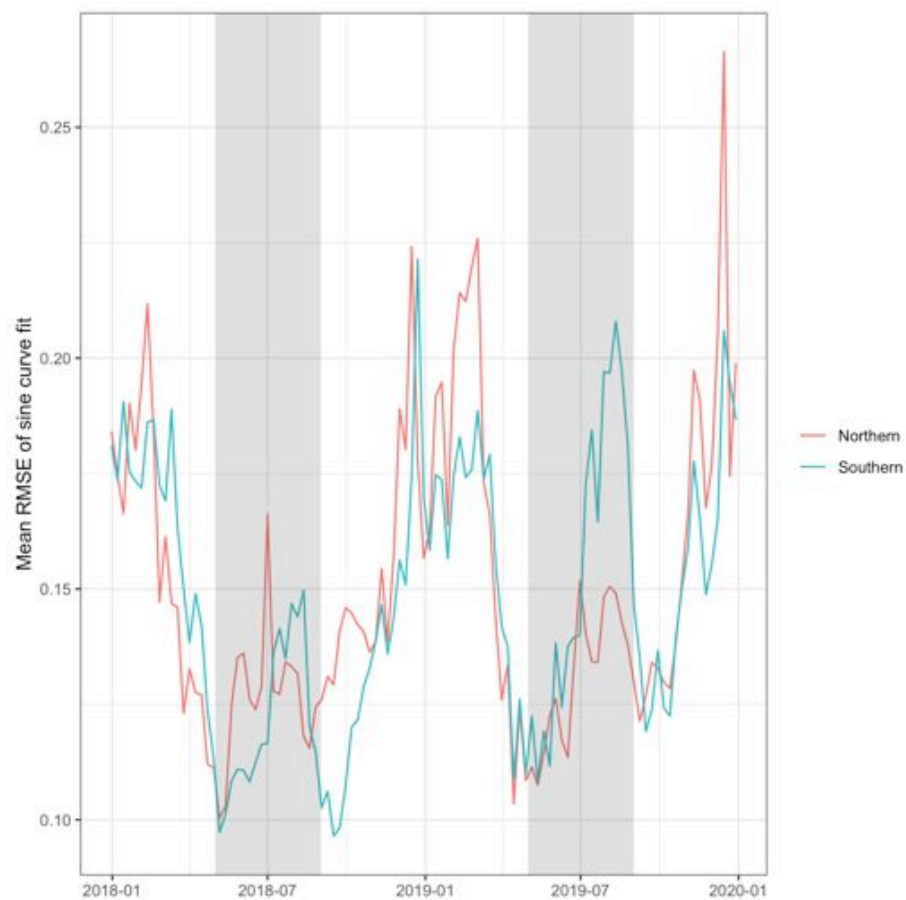


Figure 4—figure supplement 2: Model performance as measured by the root mean square error of the sine curve fit to the cluster averaged over counties within the cluster. The summer period between March and September is highlighted in light grey to emphasize the summer months.

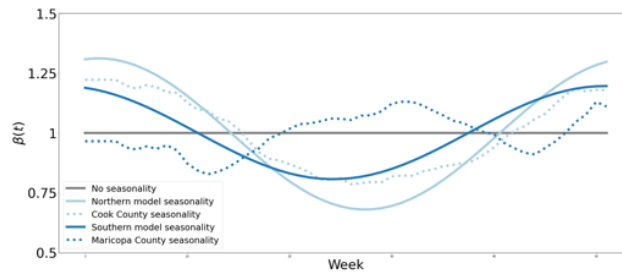


Figure 4—figure supplement 3: The seasonal forcing functions ($\beta(t)$) we used in the epidemiological model. The non-seasonal model (grey) shows no variation in transmission risk over time. We model northern seasonality via a sinusoidal model fit to the northern indoor activity data (light blue solid) and via the empirically-measured indoor seasonality from a county in the northern cluster (Cook County, light blue dotted). We model southern seasonality via a sinusoidal model fit to the southern indoor activity data (dark blue solid) and via the empirically-measured indoor seasonality from a county in the northern cluster (Maricopa County, dark blue dotted).